THE EFFECT OF COUPLED HEAVE/HEAVE VELOCITY OR SWAY/SWAY VELOCITY INITIAL CONDITIONS ON CAPSIZE MODELING

Leigh S. McCue and Armin W. Troesch
Department of Naval Architecture and Marine Engineering
University of Michigan, (USA)

Abstract

Obar *et al*. [1] described a series of model tests and a numerical model of a rectangular barge in regular beam seas with three degrees of freedom in roll, heave, and sway used to investigate the onset of capsize. The model had minimal freeboard resulting in significant water-on-deck. This paper employs the numerical model to examine specifically the impact of the coupling in heave with heave velocity initial conditions or in sway with sway velocity initial conditions on ultimate stability. Direct comparison with experimental results was used to validate the numerical model and can be found in Lee *et al* [2]-[3].

1. INTRODUCTION

One of the greatest threats to vessel safety is capsize. While capsize stability has been experimentally studied in great detail for one degree of freedom by Thompson *et al.* [4]-[5], little has been done with multiple degree of freedom experiments. This work extends the experimentation conducted by Obar *et* al. [1] and the numerical simulation and experimental structure developed by Lee *et al*. [2]-[3] to the case of coupled state variables.

Vassalos and Spyrou [6] demonstrated that combinations of effects (in their case the effect of directional instabilities on transverse stability) can dramatically alter the ultimate stability of a vehicle. Thompson and de Souza show the dependence of stability on nonlinear coupling between roll and heave [7]. While Thompson *et al* [4]-[5] as well as the work of Taylan [8] thoroughly investigate the one degree of freedom problem, Vassalos and Spyrou [6] and Thompson and de Souza [7] make clear the importance of studying combined effects.

Murashige and Aihara investigate the case of a forced flooded ship experimentally and mathematically. While they improve upon the traditional one-dimensional model through inclusion of the effects of water on deck, their model is based upon assumptions that cause one to neglect sway and heave degrees of freedom [9].

The work presented in this paper seeks to expand upon the one degree of freedom models previously discussed, and the computationally intensive models developed for fully nonlinear simulation and/or water on deck models which are currently being developed and validated [10]-[11]. This paper discusses results from a quasi-nonlinear time domain model developed by Lee [3] which is far less computationally intensive than its fully nonlinear counterparts

allowing for investigation of far greater quantities of data. Additionally, the numerical model is validated by three degree of freedom experimental results conducted at the University of Michigan Marine Hydrodynamics Laboratory [1]-[3]

Over one hundred eighty separate experiments were used in the study to validate the numerics generated by Lee *et al*. [1]-[3]. For each test case a simple box barge was excited at a frequency of 6.8 rad/s. The waves acting upon the model had a wave height to wave length ratio of 0.02. Each release, however, featured different initial conditions in roll, roll velocity, sway, sway velocity, heave, and heave velocity. These values were measured in $1/30^{th}$ of a second increments for the duration of the experimental run. Approximately 37% of the test runs resulted in capsize suggesting that initial conditions were a significant contributor to subsequent dynamics. While roll initial conditions (i.e. initial roll angle and roll velocity) are well known to influence capsize (e.g. Thompson, 1997 [5]), little has been said about heave initial conditions. A reduced-model nonlinear time-domain computer program is used in this work to provide guidance in interpreting the experimental results.

Qualitative behaviour of the capsize dynamics is presented in a number of formats. The roll phase space is characterized by "safe/unsafe basins" (e.g. Thompson [5]). These figures show capsize boundaries based upon roll initial conditions. The evolution or change of these boundaries is investigated for varying sets of heave and sway initial conditions. From similar analyses, "integrity curves" are generated for systematic variations in the initial heave displacement and heave velocity as well as sway displacement and velocity. Each point on an "integrity curve" represents the ratio of safe (i.e. non-capsize) basin area for a given wave amplitude to a similar safe basin area derived from zero wave amplitude. In this way, the integrity curves show the relative influence of incident wave excitation on capsize relative to vessel safety in the absence of incident waves.

Results from the simulation are presented here with discussions of accuracy and time of computation. Qualitative guidelines are suggested and recommendations are made for determining whether experimental programs may be sensitive to test initial conditions.

2. NUMERICAL ANALYSIS

2.1 Definition of numerical model

The works of Lee and Lee *et al* [2]-[3] develop a quasi-nonlinear three degree of freedom 'blended' hydrodynamic model to simulate highly nonlinear roll motion of a box barge. The model uses an effective gravitational field to account for the centrifugal forces due to the circular water particle motion in addition to the earth's gravitational field. This results in a local time dependent gravitational field normal to the local water surface. Additionally the model assumes long waves. Equation 1 below gives the equations of motion for the numerical model in global coordinates where a and b are added mass and damping coefficients, m and I are the mass and moment of inertia of the body, g_e is the time dependent effective gravitation, f^D are diffraction forces, ∇ is the time dependent displaced volume of water, and GZ is the ship's time dependent roll righting arm.

$$\begin{bmatrix} m+a_{22} & 0 & a_{24} \\ 0 & m+a_{33} & 0 \\ a_{42} & 0 & I_{cg}+a_{44} \end{bmatrix} \begin{Bmatrix} \ddot{x}_g \\ \ddot{y}_g \\ \ddot{\phi}_g \end{Bmatrix} +$$

$$\begin{bmatrix} b_{22} & 0 & b_{24} \\ 0 & b_{33} & 0 \\ b_{42} & 0 & b_1 \end{bmatrix} \begin{Bmatrix} \dot{x}_g \\ \dot{y}_g \\ \dot{\phi}_g \end{Bmatrix} + \begin{bmatrix} 0 & 0 & 0 \\ 0 & 0 & 0 \\ 0 & 0 & b_2 \end{bmatrix} \begin{Bmatrix} \dot{x}_g \\ \dot{y}_g \\ \dot{\phi}_g \left|\dot{\phi}_g\right| \end{Bmatrix} \quad (1)$$

$$= \begin{pmatrix} \rho g_{e_2} \nabla + f_2^D \\ \rho g_{e_3} \nabla - mg + f_3^D \\ \rho g_{e_4} GZ \nabla + f_4^D \end{pmatrix}$$

The global and body fixed coordinate systems for the model are defined in Figure 1.

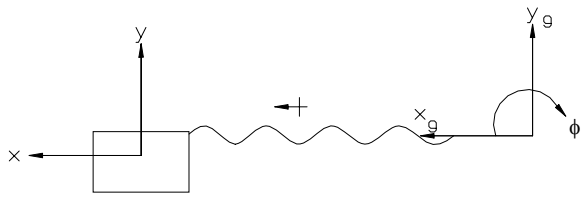

Figure 1**:** Coordinate system definition Model scale definitions: 18.25 cm draft, 1.12 cm freeboard, 66 cm length, and 30.48 cm beam.

While the numerical model cannot account for the dynamics of water on deck, such as sloshing, it does account for hydrostatic effects due to deck immergence.

The forcing due to the waves is modelled as a cosine wave. To simulate laboratory transients, the wave "ramps" from zero until steady state. An experimentally determined envelope curve was generated to create a ramped cosine wave that closely resembles the waves generated in the tank.[1] All release times for the model are defined relative to the maximum transient wave crest as shown in Figure 2 below and indicated by the notation "t_o".

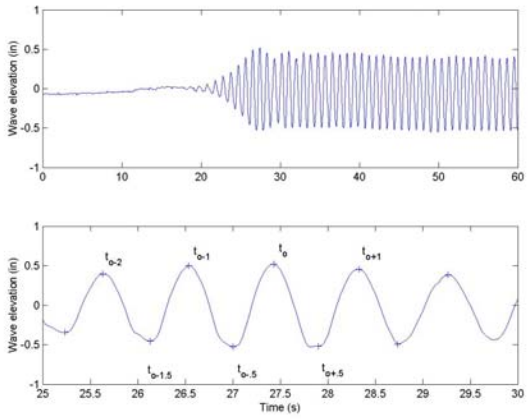

Figure 2: Sample wave profile (top) with enlarged region showing definition of points relative to t_o (bottom).

While this 'blended' model has admitted weaknesses due to the simplifications employed, it has the distinct advantage of computational efficiency. Other, multi-degree of freedom models that simulate various dynamics of water on deck run significantly slower than real time.[11] However, this model, whose results are qualitatively experimentally verified [2], runs in a fraction of the actual run time. The work that makes up this numerical study represents years worth of real time data; using this quasi-nonlinear model such data can be collected in a matter of days.

2.2 Numerical results

As discussed in the work of Soliman and Thompson [4], one can consider a set of model releases in which all initial conditions, save roll and roll velocity, are held constant. A sweep is made of roll and roll velocity initial condition pairs with conditions resulting in capsize marked in black and non capsize left white yielding a 'safe basin'. Figure 3 shows a sample safe basin generated with this numerical model (note ω_e denotes excitation frequency, ω_n represents vessel natural frequency in roll, similarly t_e and t_n represent excitation and natural periods respectively).

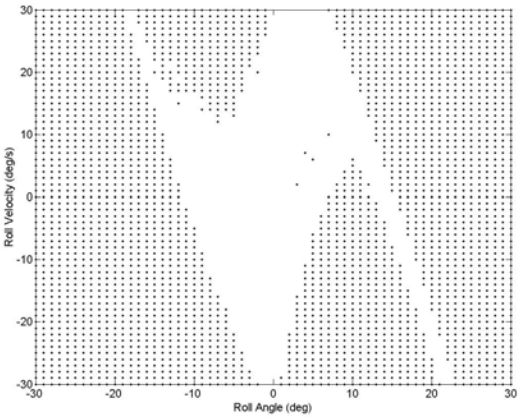

Figure 3: Safe basin for release time of t_{o-2} with sway, sway velocity, heave, and heave velocity initial conditions set equal to zero at release. $\omega_e/\omega_n \approx 3$, $h/\lambda = 0.019$.

One can then consider a set of safe basins with some third parameter varied. For example, Figure 4 shows a series of safe basins for different release times. The figure shows safe basins for 48 different release times starting from t_{o-2} until t_{o+2}. Thus a shift between two safe basins represents a 30 degree shift in phase location along the wave profile (*i.e.* 1/12 λ). This figure illustrates how crucial accurate accounting of time, and implicitly sway location, is on predicting vessel stability. Additionally, this plot demonstrates the impact transients in the incident wave profile have upon the safe basins. The safe basins before steady state, such as from t_{o-2} to $t_{o-1,}$ exhibit no periodicity (*i.e.* t_{o-2} and t_{o-1}'s safe basins are quite different), while basins from t_o to t_{o+2} produce a periodicity in that every 360 degrees of phase (or one wave length) the safe basin is virtually identical (*i.e.* $t_{o+.5}$ and $t_{o+1.5}$ are nearly the same).

It should be noted that a change in sway displacement can be explicitly written as a shift in time. For example, upon reaching steady state, a sway displacement equal to one wave length at time t_x could instead correspond to a sway displacement of zero at a time t_{x+1}, that is time moved forward through one wave period. Thus a shift in time corresponds to a change in sway displacement if time is referred to by a particular location in the wave profile, *e.g.* the maximum wave crest, t_o (Figure 2).

As described by Thompson [5], one can then introduce the idea of integrity values. Integrity is a ratio of safe area for given initial conditions to safe area for some reference case. For a typical integrity curve, wave frequency and all non-roll initial conditions would be held constant while wave amplitude is varied. As an example, Figure 5 presents an integrity curve for the box barge numerical model described in the previous section. In Figure 5 sway, sway velocity, heave, and heave velocity are all set to zero at the instant of release. A safe basin is generated for varying roll and roll velocity initial conditions (between -20 to 20 degrees and –15 to 15 degrees/sec respectively). This is done for multiple wave amplitudes with integrity values being calculated as the ratio of safe area at a particular wave height to safe area for a wave height of zero. Thus the curve begins at one. The resulting curve is an integrity curve as defined by Thompson [5] in which one notes the crucial characteristic 'Dover cliff' [5] at which point there is a distinct, rapid loss of stability. One can note that in Figure 5, integrity values are greater than one for wave amplitude to wave length ratios of 0 to approximately 0.007. Physically, integrity values greater than 1.0 indicate that the presence of waves at certain wave amplitudes can have a stabilizing effect upon the vessel relative to the zero wave condition.

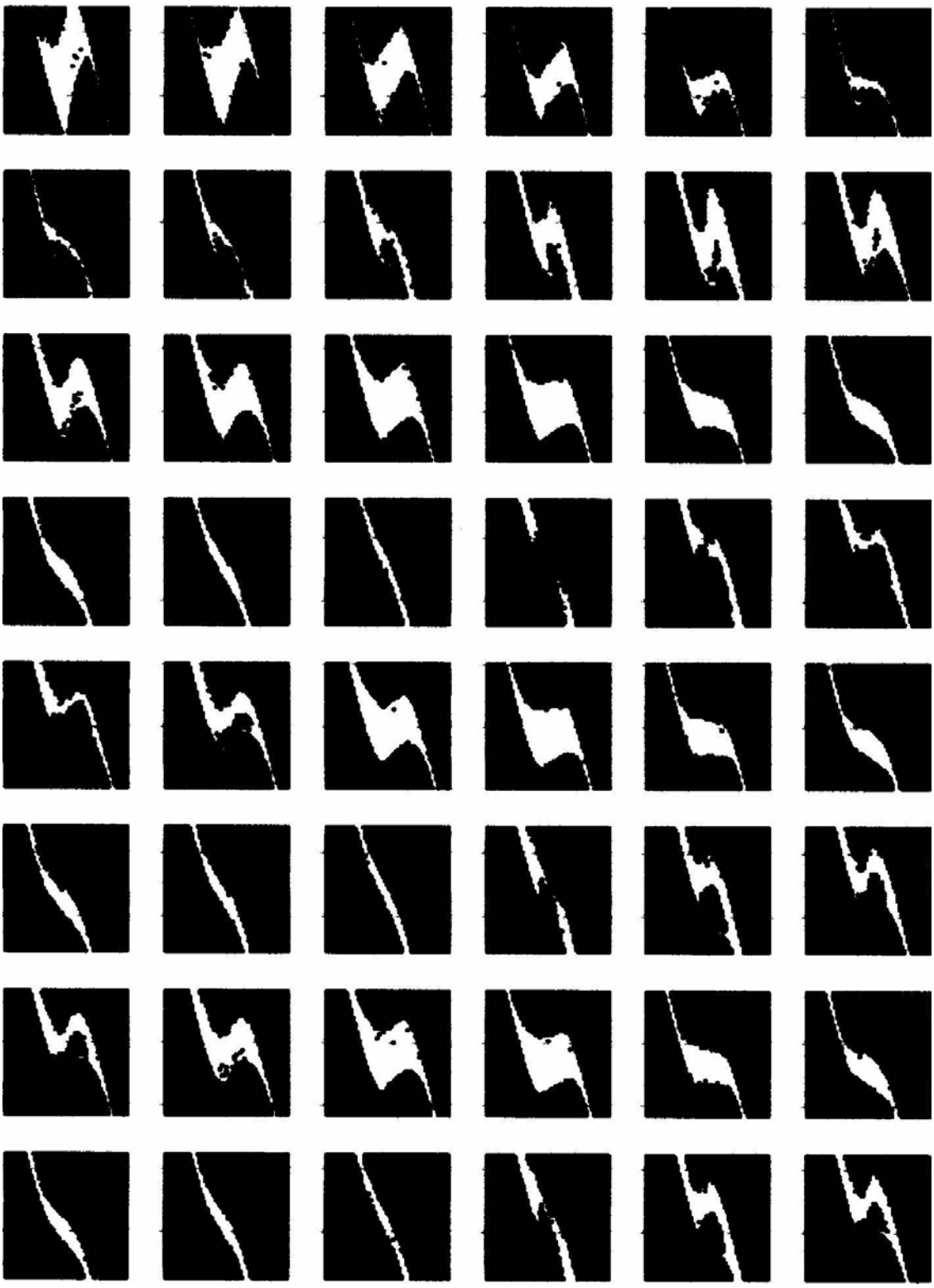

Figure 4: Safe basin for release times starting from t_{o-2} in 30 degree increments with $\tilde{\omega}_e\omega_n \approx 3$, $h/\lambda=0.019$, roll angle from -30 to 30 deg and roll velocity from -30 to 30 deg/s; *i.e.* the left hand column represents safe basins at t_{o-2}, $t_{o-1.5}$, t_{o-1}, $t_{o-.5}$, t_o, $t_{o+.5}$, t_{o+1}, and $t_{o+1.5}$. All heave and sway displacements and velocities initially set equal to zero. x and y axes represent roll and roll velocity respectively.

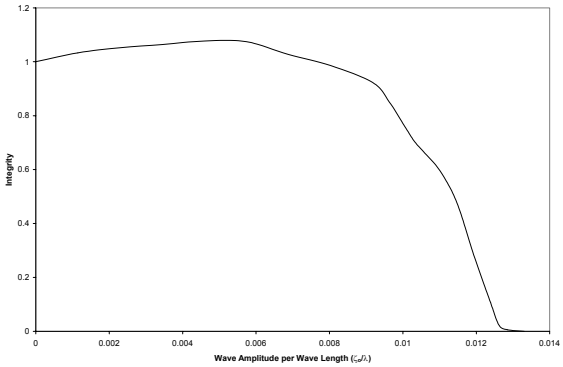

Figure 5: Integrity Curve. Sway, sway velocity, heave, and heave velocity 0 at time of release. T_e/T_n~3.

In Lee *et al* [2] a detailed study is conducted considering the ways in which these curves shift for varying initial conditions of sway, sway velocity, heave, and heave velocity. This results in series of curves such as those found in Figure 6. In this case one sees the variations in the location of the cliff; however, direct comparison is difficult as the normalization factor for each curve varies. This is analysed in detail for the 6 state variables in Lee *et al* [2].

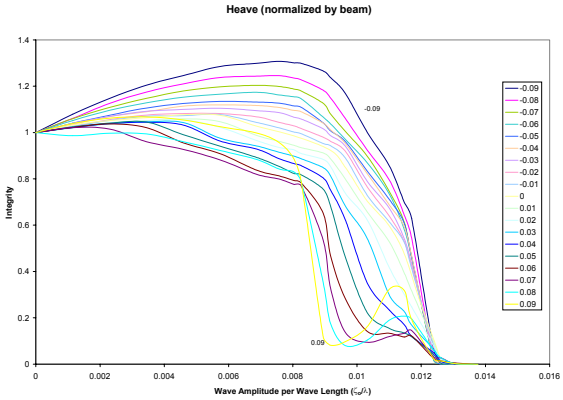

Figure 6: Heave Integrity Curves. Sway, sway velocity, and heave velocity 0 at time of release. T_e/T_n~3. Note significant change with respect to heave in location of cliff on curve but not in x-axis intercept (location where integrity is zero).

While this lends great insight into anticipated behaviour from individual state variable variations, it still cannot fully capture the idiosyncrasies of experiments as there is no graphic coupling amongst the remaining state variables, sway, sway velocity, heave, and heave velocity.

Therefore, instead of viewing the parameters as integrity curves, one can consider a surface, in which integrity (defined on the roll and roll velocity phase space plane) for a fixed wave amplitude is calculated for pairings of two other state variables such as sway and sway velocity (Figure 7) or heave and heave velocity (Figure 8). Each of these surfaces is for a fixed wave height and frequency (h/λ=.019 and $\omega_e/\omega_n \approx 3$) and is normalized such that the integrity value is 1 when sway, sway velocity, heave, and heave velocity are zero.

Figure 7 presents a three dimensional integrity surface where each point is an integrity value representing the ratio of safe area to unsafe area for a roll/roll velocity grid as a function of sway and sway velocity. Heave and heave velocity are defined as zero at the time of release. Additionally excitation frequency and incident wave amplitude are constants. This figure clearly shows the relative independence of stability on sway velocity initial conditions. If one were to pick a fixed value of sway the plot collapses to a two-dimensional curve representing integrity as a function of sway velocity. This curve is relatively horizontal and constant thus showing the independence of integrity on sway velocity. For example, for sway equal to one wave length (or correspondingly zero wave length), the maximum integrity value as a function of sway velocity is 1.24 and the minimum is 0.70. While this is non-trivial, comparatively speaking, this is a relatively small change in contrast to the effects seen by changes in sway displacement, heave displacement, and heave velocity.

If one were to instead consider a constant sway velocity, we see integrity values as a function of sway vary from zero to 2.2. Therefore one can see that for any fixed sway velocity value, there is a strong dependence of the integrity value upon sway position. In fact, for values of sway from approximately .15λ to .65λ the integrity values are zero irregardless of sway velocity. This indicates for some initial release positions on a wave (the region 15%-65% of a wave length beyond a peak) the vessel shall always capsize regardless of initial roll angle, initial roll velocity, or sway velocity for a wave amplitude to wave length ratio of 0.0096 and an excitation frequency to natural frequency ratio of approximately 3. This is due to the fact that this wave amplitude is in a particularly steep region of the integrity curve. Referring to Figure 5, one should note the steep drop off at approximately ζ_o/λ=.01. For a set of sway integrity curves the location of this 'cliff' is relatively invariant. More details on this are given by Lee *et al* [2].

Figure 8 demonstrates the intricate interdependence between heave and heave velocity state variables in determining ultimate vessel stability. For the surface presented in Figure 8 sway and sway velocity are zero at the time of release and wave height and frequency are constants for each point determining the surface. It should be noted though that after the time of release the vessel is unconstrained in all three degrees of freedom, thus sway and sway velocity are allowed to evolve in time just as heave, heave velocity, roll and roll velocity evolve. This is true for the data comprising both Figures 7 and 8.

Unlike Figure 7 we note there are no similar statements we can make regarding a relative independence. Both heave and heave velocity have substantial influence on the ultimate state of the vessel and a coupling between the two conditions of heave and heave velocity can significantly alter the location of the vessel on such an integrity surface indicating a dramatic shift in vessel safety. Only generally can we say that maximum integrity values occur when heave velocity initial conditions are near zero for all heave.

3. CONCLUSIONS

This paper presents the results of a thorough computational study into the interdependence of initial conditions in multiple degrees of freedom on predicting ultimate state of a simple box barge. While the hydrodynamic model is highly simplified it serves as a useful tool having demonstrated the influence coupled degrees of freedom can have on capsize prediction.

The final two figures, 7 and 8, demonstrate the dependence of vessel stability on heave, heave velocity, sway and to a lesser extent sway velocity. While many models used in the present day literature focus upon one degree of freedom or a reduced order model, this work has shown that such models can be vulnerable to neglecting crucial dynamics.

It is not sufficient to consider simply one state variable such as roll angle nor two state variables models coupling roll with roll velocity. This work demonstrates that elaborate couplings of multiple state variables in roll, sway and heave can significantly alter predictions of safe versus capsize and thus one must exercise care in the use of reduced order models.

4. ACKNOWLEDGEMENTS

The authors would like to acknowledge the support of the National Defense Science and Engineering Graduate Fellowship program for sponsoring this research. Additionally the authors would like to thank Young-Woo Lee and Michael Obar whose work laid the basis for this paper.

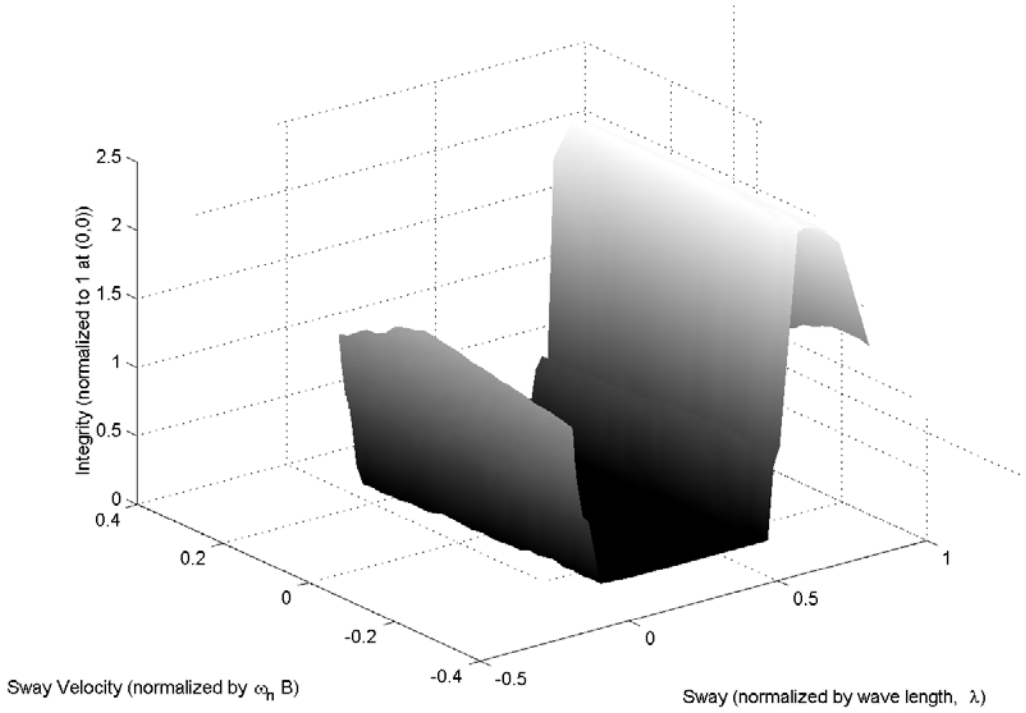

Figure 7: Sway/sway velocity integrity surface. Heave and heave velocity 0 at time of release, t_o. $\omega_e/\omega_n \approx 3$, $h/\lambda = 0.019$.

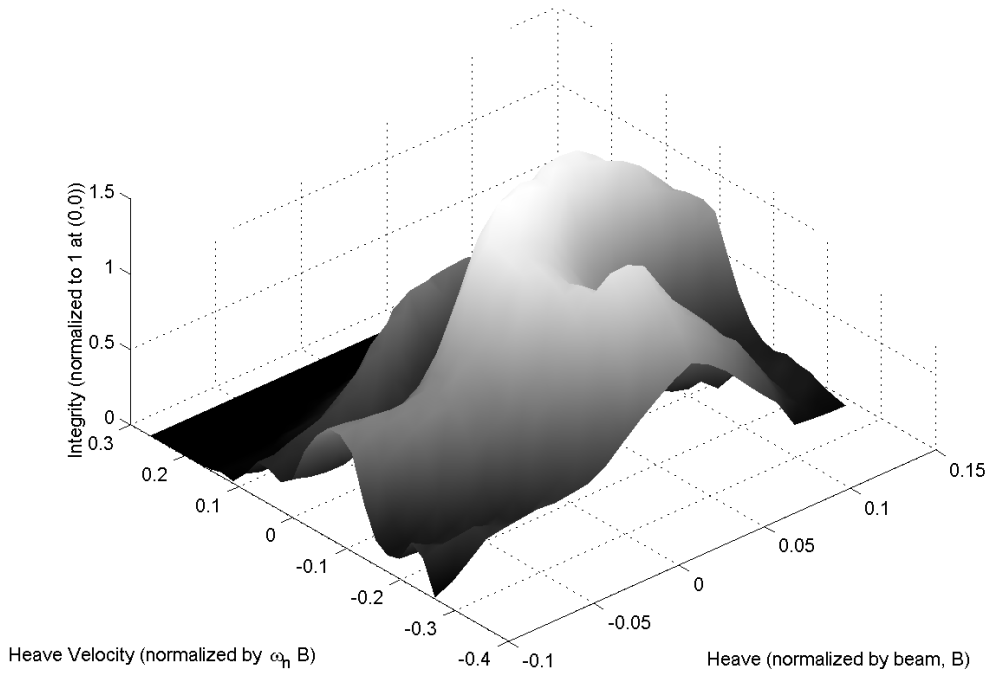

Figure 8: Heave/heave velocity integrity surface. Sway and sway velocity 0 at time of release, t_o. $\omega_e/\omega_n \approx 3$, $h/\lambda = 0.019$.

5. REFERENCES

[1] Obar, M., Y.-W. Lee, and A. Troesch, 'An experimental investigation into the effects initial conditions and water on deck have on a three degree of freedom capsize model,' Proceedings of the Fifth International Workshop on the Stability and Operational Safety of Ships, September 2001.

[2] Lee, Y-W, L. McCue, M. Obar, and A. Troesch, 'Experimental and numerical investigation into the effects of initial conditions on a three degree of freedom capsize model,' submitted to *Journal of Ship Research*, 2003.

[3] Lee, Young-Woo, 'Nonlinear ship motion models to predict capsize in regular beam seas,' Doctoral dissertation, Department of Naval Architecture and Marine Engineering, University of Michigan, Ann Arbor, MI, 2001.

[4] Soliman and Thompson, 'Transient and steady state analysis of capsize phenomena', *Applied Ocean Research*, 1991.

[5] Thompson, J., 'Designing against capsize in beam seas: Recent advances and new insights,' *Appl Mech Rev*, 50, 5, May 1997.

[6] Vassalos, D. and K. Spyrou, 'An investigation into the combined effects of transverse and directional stabilities on vessel safety,' Fourth International Symposium on the Stability of Ships and Ocean Vehicles, Naples, Italy, pp. 519-527.

[7] Thompson, J.M.T and J.R. de Souza, 'Suppression of escape by resonant modal interactions: in shell vibration and heave-roll capsize.' *Proceedings of the Royal Society of London*, A452, 1996, 2527-2550.

[8] Taylan, M. 'Static and dynamic aspects of a capsize phenomenon,' *Ocean Engineering*, Vol 30, 2003, pp 331-350.

[9] Murashige, Sunao and Aihara, Kazuyuki, 'Coexistence of periodic roll motion and chaotic one in a forced flooded ship,' *International Journal of Bifurcation and Chaos*, Vol. 8, No. 3, 1998, pp 619-626.

[10] Huang, J., Cong, L., Grochowalski, S., and Hsiung, C.-C., 'Capsize analysis for ships with water shipping on and off the deck,' Twenty-Second Symposium on Naval Hydrodynamics, Washington, D.C., 1999.

[11] Belenky, V, D. Liut, K Weems, and Y-S Shin, "Nonlinear ship roll simulation with water-on-deck," Proceedings of the 2002 Stability Workshop, Webb Institute.